Journal of Applied Polymer Science

Design of hemocompatible poly(DMAEMA-*co*-PEGMA) hydrogels for controlled release of insulin

Lemmuel L. Tayo,[1,2] Antoine Venault,[1] Vryan Gil R. Constantino,[1,2] Alvin R. Caparanga,[2] Arunachalam Chinnathambi,[3] Sulaiman Ali Alharbi,[3] Jie Zheng,[4] Yung Chang[1,3]

[1]R&D Center for Membrane Technology, Department of Chemical Engineering, Chung Yuan Christian University, Chung-Li, Taoyuan 320, Taiwan

[2]School of Chemical Engineering and Chemistry, Mapúa Institute of Technology, Intramuros, Manila 1002, Philippines

[3]Department of Botany and Microbiology, College of Science, King Saud University, Riyadh 11451, Kingdom of Saudi Arabia

[4]Department of Chemical and Biomolecular Engineering, University of Akron, Akron, OH 44325

Correspondence to: A. Venault (E-mail: avenault@cycu.edu.tw) and Y. Chang (ychang@cycu.edu.tw)

ABSTRACT: This works aims at (i) studying the antiadhesive properties and the hemocompatibility of poly[2-(dimethylamino)ethyl methacrylate]-*co*-poly[(ethylene glycol)methacrylate] [poly(DMAEMA-*co*-PEGMA)] copolymers and (ii) investigating the insulin delivery kinetics through hydrogels at physiological pH. A series of poly(DMAEMA-*co*-PEGMA) hydrogels have been synthesized, and their controlled composition was confirmed by X-ray photoelectron spectroscopy. Then, antibiofouling properties of hydrogels—fibrinogen, erythrocytes, and thrombocytes adhesion—are correlated to their molecular compositions through their hydrophilic properties. As DMAEMA/PEGMA ratio of 70/30 (D70) offers the best compromise between pH sensitivity and hemocompatibility, it is selected for investigating the kinetic rate of insulin release at physiological pH, and the diffusion coefficient of insulin in gel is found to be 0.64×10^{-7} cm^2 s^{-1}. Overall, this study unveils that poly(DMAEMA-*co*-PEGMA) copolymers are promising hemocompatible materials for drug delivery systems. © 2015 Wiley Periodicals, Inc. J. Appl. Polym. Sci. **2015**, *132*, 42365.

KEYWORDS: biocompatibility; biomedical applications; biomaterials; copolymers; gels

Received 4 March 2015; accepted 13 April 2015

DOI: 10.1002/app.42365

INTRODUCTION

Drug delivery is a rapidly expanding discipline in which the main goal is to enable temporal and spatial control release of therapeutic agents inside a biological system. The potency of pharmaceuticals may depend on the drug delivery system used. Therefore, their careful design can improve the efficiency of medical treatments while minimizing side effects.[1] Polymeric networks and hydrogels are considered as ideal drug/gene delivery systems because many of them, the so-called stimuli responsive, can adapt their spatial configuration to the environment they face,[2,3] which eventually ensures a controllable delivery rate. Among them, those containing dimethylaminoethyl methacrylate (DMAEMA) moieties are popular as this block is pH responsive, which offers the possibility to deliver dugs in specific regions of the organism when oral administration is the chosen route. The combination of DMAEMA with HEMA- or PEG-derivative blocks, as reviewed in Table I, also shows great potential, as HEMA and PEG are common effective nonfouling blocks and help at improving the biocompatibility of synthetic materials.[4–15] In general, a drug delivery system with nonfouling moieties and environment-responsive blocks has improved biocompatibility and can trigger drug release.

Optimizing the biocompatibility of a polymer matrix to be used as a drug delivery system consists of carefully studying the potential interactions of the materials with human proteins or cells. The target is to minimize interactions and to prevent immune response and uncontrolled release of the therapeutic agent. In particular, the designed materials should efficiently resist the adhesion of plasma proteins, such as fibrinogen, which can mediate platelet activation and blood clotting,[16–18] as well as the direct interactions with blood cells. As shown in Table I, if PEG derivatives have been combined with DMAEMA, there is a clear lack of data on the hemocompatibility of such systems, which suggests the need for further investigation. Poly(ethylene glycol)methyl ether methacrylate (PEGMA) moieties have been proven to provide surfaces with hemocompatible properties in a series of recent work on the design of hemocompatible PVDF membranes.[19,20] Therefore, the polymeric system earlier presented by Fournier *et al.*[6] could be promising as a biocompatible drug delivery material. Yet, major differences in

Table I. Polymeric Matrices Containing DMAEMA and PEG Moieties

Reference	Polymer	Stimulus tested	Nonfouling test(s)	Loaded drug/gene
Loizou *et al.*[4]	DMAEMA-*b*-PEGMA-*b*-DMAEMA[a]	pH	/	/
Brahim *et al.*[5]	p(HEMA-DMAEMA)[b]	pH	/	Insulin
				Protamine
Fournier *et al.*[6]	P(DMAEMA-*stat*-PEGMA)[c]	pH	/	/
		Temperature		
Lin *et al.*[7]	PEG-*a*-PDMAEMA[d]	pH	BSA	Plasmid DNA
			Red blood cells	
Cerda-Cristerna *et al.*[8]	Linear PDMAEMA	/	/	/
	Poly(DMAEMA-*block*-MAPEG)[e]			
	Poly(DMAEMA-*random*-MAPEG)			
Zhu *et al.*[9]	PDMAEMA-*SS*-PEG-*SS*-PDMAEMA[f]	/	/	Plasmid DNA
Nelson *et al.*[10]	PEG-(DMAEMA-*co*-BMA)[g]	pH	Red blood cells	siRNA
Zhu *et al.*[11]	ss-PHPA-*g*-P(DMAEMA)[h]	/	/	Plasmid DNA
Lundy *et al.*[12]	Poly[(HPMA-*co*-PDSMA)-*b*-(PAA-*co*-MAEMA-*co*-BMA)][i]	/	/	siRNA
Cho *et al.*[13]	Star polymer of DMAEMA and EGDMA[j]	/	/	siRNA/pDNA
Lee *et al.*[14]	Poly[(HEMA-BA)-*co*-(DMAEMA-CCDP)][k]	pH	Hela cells	/
		Redox potential		
Li *et al.*[15]	PEG_{20k}–peptide–pDMAEMA	/	/	siRNA
This work	Poly(DMAEMA-*co*-PEGMA)	pH	Plasma proteins	Insulin
			Red blood cells	
			Platelets	

[a] (*N*,*N*-(Dimethylamino)ethyl methacrylate)-*block*-poly(ethylene glycol)methyl ether methacrylate-*block*-(*N*,*N*-(dimethylamino)ethyl methacrylate).
[b] Poly(2-hydroxyethyl methacrylate-*N*′,*N*′-dimethylaminoethyl methacrylate).
[c] Poly[(*N*,*N*-(dimethylamino)ethyl methacrylate)-*stat*-poly(ethylene glycol)methyl ether methacrylate].
[d] Poly(ethylene glycol) and poly[2-(dimethylamino)ethyl methacrylate] connected through a cyclic ortho ester linkage.
[e] Poly[(2-dimethylamino-ethylmethacrylate)-*block*-(PEG α-methoxy, ω-methacrylate)].
[f] Poly-(dimethylaminoethyl methacrylate)-*SS*-poly(ethylene glycol)-*SS*-poly-(dimethylaminoethyl methacrylate).
[g] Poly[(ethylene glycol)-*b*-{[2-(dimethylamino)ethyl methacrylate]-*co*-(butyl methacrylate)}.
[h] *SS*-Poly(*N*−3-hydroxypropyl)aspartamide-*graft*-poly[2-(dimethylamino)ethyl methacrylate].
[i] Poly[*N*-(2-hydroxypropyl)methacrylamide-*co*-*N*-(2-(pyridin-2-yldisulfanyl)ethyl)methacrylamide)-*block*-(propylacrylic acid-*co*-dimethylaminoethyl methacrylate-*co*-butyl methacrylate)].
[j] Ethylene glycol dimethacrylate.
[k] Poly[(hydroxyethyl methacrylate-*g*-benzoic acid)-*co*-(dimethylaminoethyl methacrylate-*g*−2-chloro-3′,4′-dihydroxyacetophenone)].

the polymer chain organization, entanglement, and surface density arise from the preparation process and the state (gel, dry membrane, etc.) of the polymer material. In other words, if polystyrene-*block*-PEGMA permitted to importantly improve the blood compatibility of dry films, this result cannot be extrapolated to hydrogel networks and careful dedicated tests should be run. In this respect, if the work of Fournier *et al.* offered important perspectives for the use of poly(DMAEMA-*stat*-PEGMA) polymers, it should be completed. Hydrophilicity is another essential property of these systems that was obtained from surface energy measurements.[6] Hydrophilicity is generally accepted as a prerequisite for a material to perform low-biofouling properties.[21] Therefore, it is believed that hydrogels containing controlled ratio of DMAEMA/PEGMA moieties should present adequate hemocompatibility. The optimal ratio has yet to be determined. Additionally, the effectiveness of such material as a drug-release system should be tested.

Inspired from the work of Fournier *et al.*, we have designed poly(DMAEMA-*co*-PEGMA) hydrogels. As they did not prepare hydrogels, we first characterized the chemical properties of the as-prepared polymer matrices, as our first aim is to demonstrate that the preparation process is well controlled. Then, we move onto the assessment of the biocompatibility of gels by evaluating the resistance of hydrogels to the adhesion of plasma proteins, as well as their ability to repel platelets and erythrocytes. Finally, we put efforts on the understanding of kinetic release of insulin, a model drug as that used by Brahim *et al.*[5] administrated to

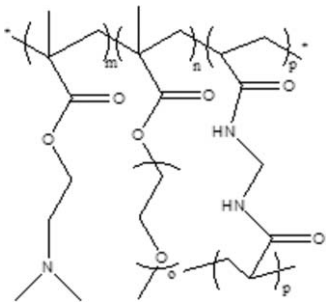

Scheme 1. Chemical structure of poly(DMAEMA-*co*-PEGMA) hydrogels.

diabetic patients, and characterize its diffusivity through the hydrogel system. This study not only introduces new insight of intelligent hemocompatible PEGylated hydrogels, but also provides a fundamental understanding of properties at play in the controlled release of insulin.

EXPERIMENTAL

Materials

The monomer 2-(dimethylamino)ethyl methacrylate (DMAEMA, 99%) and the crosslinker *N*,*N*′-methylenebisacrylamide (NMBA, 96% extra pure) were obtained from Acros Organics. The comonomer PEGMA with a molecular weight of 475 g mol^{-1} was purchased from Aldrich. The initiators *N*,*N*,*N*′,*N*′-tetramethylethylenediamine (TEMED) and ammonium peroxodisulfate (APS) were acquired from Alfa Aeser. Deionized (DI) water used in the experiments was purified using Millipore water purification system with 18.0 MΩ cm minimum resistivity.

Preparation of Hydrogels

Deionized water and DMAEMA were mixed in a glass vial with constant stirring at 320 rpm. The crosslinker NMBA was added and kept cool in ice bath while maintaining the rate of stirring. The initiators APS and TEMED were added in the solution. The resulting mixture was immediately transferred by means of a syringe in between a pair of glass plates separated by a silicone rubber spacer with 0.2 mm thickness. The reaction was allowed to proceed at room temperature for several hours. After polymerization, gels were immersed in large amounts of water for 48 h to remove chemical residues. The formed hydrogels were punched (10 mm biopsy punch; Acuderm, FL) into disks of 10.0 mm diameter and 0.2 mm thickness. This was stored in DI water before its usage. Pure DMAEMA and PEGMA hydrogels were prepared using a similar procedure except that the other polymer was excluded from the reaction. The chemical structure of crosslinked poly(DMAEMA-*co*-PEGMA) is presented in Scheme 1, and the compositions of the synthesized hydrogels are summarized in Table II.

Characterization of Hydrogels

The actual compositions of the poly(DMAEMA-*co*-PEGMA) hydrogels were determined using X-ray photoelectron spectroscopy (XPS). XPS measurements were made using a Thermal Scientific K-Alpha spectrometer equipped with a monochromated Al K X-ray source (1486.6 eV photons). The energy of emitted electrons was measured with a hemispherical energy analyzer at pass energies ranging from 50 to 150 eV. All data were collected at a photoelectron take-off angle of 0° with respect to the sample surface. The binding energy (BE) scale is referenced by setting the peak maximum in the C 1s spectrum to 284.6 eV. The high-resolution C 1s spectrum was fitted using a Shirley background subtraction and a series of Gaussian peaks. The quantified mole fraction of poly(DMAEMA) (X_{DMAEMA}) in the poly(DMAEMA-*co*-PEGMA) hydrogels was determined based on the spectral area ratio of the atomic percentages of the N 1s of the poly(DMAEMA) amine group and C 1s and O 1s of both the poly(DMAEMA) and PEGMA at a BE of ~ 399, 284, and 531 eV, respectively. The results of the XPS are summarized in Table II. Surface contact angles of prepared hydrogels were measured with an angle meter (Automatic Contact Angle Meter, Model CAVP, Kyowa Interface Science,

Table II. Characteristics of Poly(DMAEMA-*co*-PEGMA) Hydrogels

	Reaction ratios of comonomers (mol %)[a]		Compositions of hydrogels (wt %)[b]		Characterization of crosslinked hydrogels[c]		
Sample ID	DMAEMA	PEGMA	DMAEMA	PEGMA	X_{DMAEMA}	Swelling ratio	Contact angle
D0-P100	0	100	0	100	0	7.34	149.45
D20-P80	20	80	8	92	0.26	8.25	137.74
D50-P50	50	50	25	75	0.57	8.09	126.21
D70-P30	70	30	43	57	0.73	11.62	124.05
D80-P20	80	20	57	43	0.84	14.69	119.45
D90-P10	90	10	75	25	0.91	21.19	114.98
D100-P0	100	0	100	0	1	35.25	110.59

[a] Reaction mole ratios of DMAEMA and PEGMA monomers used with fixed total monomer mass percentage of 20 wt % in the prepared reaction solution.
[b] The theoretical compositions of the poly(DMAEMA-*co*-PEGMA) hydrogels were calculated based on reaction ratios and molecular weight of comonomers.
[c] The mole fraction of poly(DMAEMA) (X_{DMAEMA}) in the crosslinked poly(DMAEMA-*co*-PEGMA) hydrogels was determined by XPS in the dry state based on the spectral area ratio of the atomic percentages of the N 1s of the DMAEMA amine group and C 1s and O 1s of both the DMAEMA and PEGMA of ~ 399, 284, and 531 eV, respectively. Swelling ratios of equilibrated hydrogel disks were estimated in deionized water at 25°C. Surface contact angles of prepared hydrogels were measured with an angle meter using diiodomethane in H_2O at 37°C.

Japan) at 37°C. Diiodomethane was dropped on the sample surface under water medium at three different sites. The average of the measured values for each of the prepared hydrogels from five independent disks was taken as its contact angle.

pH Sensitivity of Hydrogels

Hydrogel disks were dried in a vacuum oven for 24 h. The oven temperature and pressure were set to 40°C and 20 cmHg, respectively. After every hour, the pressure was decreased by 20 cmHg until it reached 70 cmHg vacuum. Drying of hydrogels was continued until constant weight was attained. The dry weights of each hydrogel were recorded as W_d. The hydrogels were placed in different 24-well plates where 1 mL of acidic or basic solution at varying pH was added to each well. After 24 h of soaking, the wet weights of hydrogels were recorded as W_w. All measurements were done in triplicates, and the average of these values together with their standard deviations was reported. The swelling ratio (R) was computed using the following equation:

$$R = \frac{W_w - W_d}{W_d}. \quad (1)$$

Plasma Protein Adsorption

Enzyme-linked immunosorbent assay (ELISA) was used to evaluate the adsorption of fibrinogen in human plasma on the surface of the hydrogel. Disks (with surface area of 0.785 cm^2) were placed in individual wells on a tissue culture plate, equilibrated with 1 mL of phosphate buffered solution (PBS), and soaked in 1 mL of 100% platelet-poor plasma solution. To block the protein-unoccupied surface of the hydrogel disks, bovine serum albumin (BSA, purchased from Aldrich) was mixed for 90 min and rinsed with PBS. Primary monoclonal antibodies were added to the disks and subsequently incubated with the secondary monoclonal antibody, horseradish peroxidase-conjugated immunoglobulins, for 60 min. The hydrogel disks were rinsed five times with 1 mL PBS and transferred into clean wells, followed by the addition of 500 μL PBS containing 1 mg mL^{-1} 3,3′,5,5′-tetramethylbenzidine as a chromogen, 0.05 wt % Tween 20, and 0.05 wt % hydrogen peroxide. The enzyme-induced color reaction was controlled for 5 min and immediately stopped by adding 500 μL of 1 mmol mL^{-1} H_2SO_4 to each well. Light absorbance was measured at 450 nm using a microplate reader. ELISA measurements were repeated using six independent disks for each hydrogel composition, and then the average values were reported. All reactions in this assay were done at a constant temperature of 37°C.

Blood Platelet Adhesion

The hydrogel disks (0.785 cm^2 surface area) were placed in individual wells on a 24-well tissue culture plate, and each well was equilibrated with 1000 μL of PBS for 180 min at 37°C. Blood was obtained from a healthy human volunteer. Platelet-rich plasma solution containing 10^5 blood cells per milliliter was prepared by centrifugation of blood at 20 Hz (1200 rpm) for 10 min. Platelet concentration was determined by microscopy (NIKON TS 100F). A total of 1000 μL of the platelet suspension plasma was placed on the hydrogel surface in each well of the tissue culture plate and incubated for 120 min at 37°C. After the hydrogel disks were rinsed twice with 1000 μL of PBS, they were immersed into 2.5% glutaraldehyde of PBS for 48 h at 4°C to fix the adhered platelets and adsorbed proteins. Then, hydrogels were rinsed twice with 1000 μL of PBS and gradient-dried with ethanol in 95, 85, 75, 50, 25, 5, and 0% v/v PBS for 5 min in each step and air-dried. Finally, the samples were sputter-coated with gold prior to observation under JEOL JSM-5410 scanning electron microscopy (SEM) operating at 7 keV. Adhering platelets were counted from SEM images at 1000× magnification from five different areas on hydrogel disks.

Kinetics of Insulin Release

Insulin was loaded into the precut hydrogel by imbibition. Hydrogels were first dried in the same manner as previously discussed (drying for determination of the pH swelling ratio). Then, a concentrated solution of insulin (1 mg mL^{-1}) was prepared in an acetate buffer (0.1*M*, pH 3.5). The dried hydrogels were then soaked in this solution for 24 h at room temperature. The weight of insulin loaded into the solution was determined by measuring the difference between the weight of the freshly cut hydrogel (prior to insulin loading) and that of the insulin-loaded hydrogel. The amount of loaded insulin was computed by considering the density of the insulin solution and its concentration in the solution which is 1 mg mL^{-1}. Hydrogels were again dried in the same manner as previously discussed. After drying, the hydrogels were submerged in phosphate buffer saline (0.1*M*, pH 7.4). The amount of released insulin in the media was determined at different time points and was quantified using UV–vis spectrophotometer set at 200 nm (determined from the whole range scan for insulin). The volume of the solution was maintained by returning back the aliquots after measurements were made.

RESULTS AND DISCUSSION

Chemical Analysis of Hydrogels

XPS analysis can determine elemental composition of hydrogels by measuring relative abundance of specific chemical bonds from the spectra (Figure 1). This analytical technique can quantify the major polymer components in the hydrogel. One approach makes use of measuring spectral area ratio of atomic percentages of N 1s from DMAEMA amine groups and that of C 1s and O 1s from both DMAEMA and PEGMA from each hydrogel spectrum. The results of this analysis and the calculated amounts of DMAEMA are summarized in Table II. Another approach involves identification of carbon bonds. The C 1s core-level spectrum of the hydrogel can be curve-fitted to peak components for C—O, C═O, C—C, and C—N bonds at different binding energies of 286.1, 288.4, 284.6, and 286.4 eV, respectively, as observed from Figure 2. The relative amounts of the chemical bonds C—O, C═O, C—C, and C—N can be determined by computing the area of each curve relative to the entire area of all the curves. The analyses of the curve-fitted data in Figure 2 for C 1s core-level spectrum are shown in Table III. The results in Table II show small deviations between the theoretical and actual amounts of DMAEMA in each hydrogel from XPS analysis. The graph in Figure 2 and the data on Table III are consistent with the above observations. Actual ratios of the chemical bonds CO/CN and C═O/CN were slightly smaller than the theoretical values. It has been previously reported that

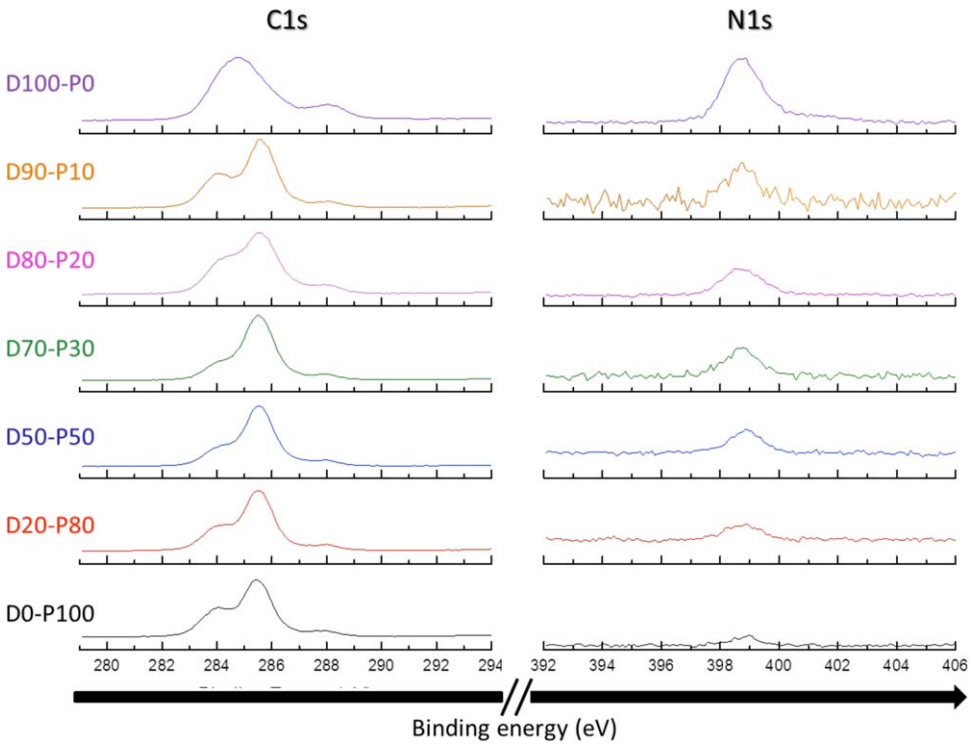

Figure 1. XPS spectra of the poly(DMAEMA-*co*-PEGMA) hydrogels. [Color figure can be viewed in the online issue, which is available at wileyonlinelibrary.com.]

during polymerization process, pi bonds in the DMAEMA molecule are cleaved faster than PEGMA. Therefore, there is a higher probability for DMAEMA to be incorporated first into the hydrogel when compared with PEGMA. This rationalizes why the actual amount of DMAEMA is slightly higher than the theoretical amount.[6]

Swelling Behavior of Hydrogels

The swelling behavior was determined by measuring the amount of water absorbed by each hydrogel. Figure 3(a) shows the swelling response of each hydrogel composition relative to the amount of DMAEMA. The results indicate that the swelling ratio of the hydrogel increases with DMAEMA content. DMAEMA is primarily responsible for water absorption because it contains functional groups that have the ability to entrap water molecules by hydrogen bonding. Figure 3(b) shows the different values of the swelling ratios of the hydrogels at various pH. There is a consistent decrease in the swelling ratios of all copolymers and pure DMAEMA hydrogels as pH increases. The results in Figure 3(b) also show the unresponsive behavior of PEGMA at different pH. This important property can be used to finely tune the desired swelling of pH-responsive biopolymers for a variety of applications. Generally, the swelling response of hydrogels at various pH depends on the presence of ionizable functional groups.[22] The nitrogen in the amine group in DMAEMA can be protonated at low pH and cause internal swelling within the polymer. The repulsive nature of these groups will lead to the overall swelling of the entire structure. At high pH, amine groups are less ionized, charge repulsion is minimized, and the polymer interaction is increased leading to a "collapsed" state.[23–25] It can be seen in Figure 3(b) that the swelling ratio of the hydrogel changes drastically within the pH range from 3.0 to 5.0, which suggests its pK_a range, along with a pulsatile behavior.[26]

Resistance to Nonspecific Protein Adsorption

Biocompatibility is a property wherein the material elicits little or no immune response to the organism or the material can be integrated to a particular tissue without rejection.[27–29] Numerous researchers in the field of drug delivery have attempted to find the ideal biocompatible material for specific applications.[5,30–36] One of the important factors in biocompatibility is protein adsorption on the hydrogel. Generally, proteins adsorb greater on hydrophobic surfaces. In our study, ELISA was used to quantify the adsorbed fibrinogen. Fibrinogen is a protein responsible for blood clotting or coagulation. The current practice is to simply coat a surface with a hydrophilic material or to increase the hydrophilicity of a material to lessen protein adsorption on the surface. Measuring the diiodomethane contact angle permits to evaluate the hydrophilicity of hydrogel surfaces. The higher its value, the more hydrophilic is the surface.[37–39] Figure 4 shows a plot of the corresponding diiodomethane contact angle of each hydrogel and the amount of adsorbed proteins measured using ELISA. It can be observed that the relative protein adsorption is low when the contact angle is high. Hydrophilic materials are less prone to protein adsorption and are more biocompatible. Although both DMAEMA and PEGMA contain polar functional groups, they greatly differ in the degree of the hydrophilicity. In Figure 4, it can be seen that as the concentration of DMAEMA increases,

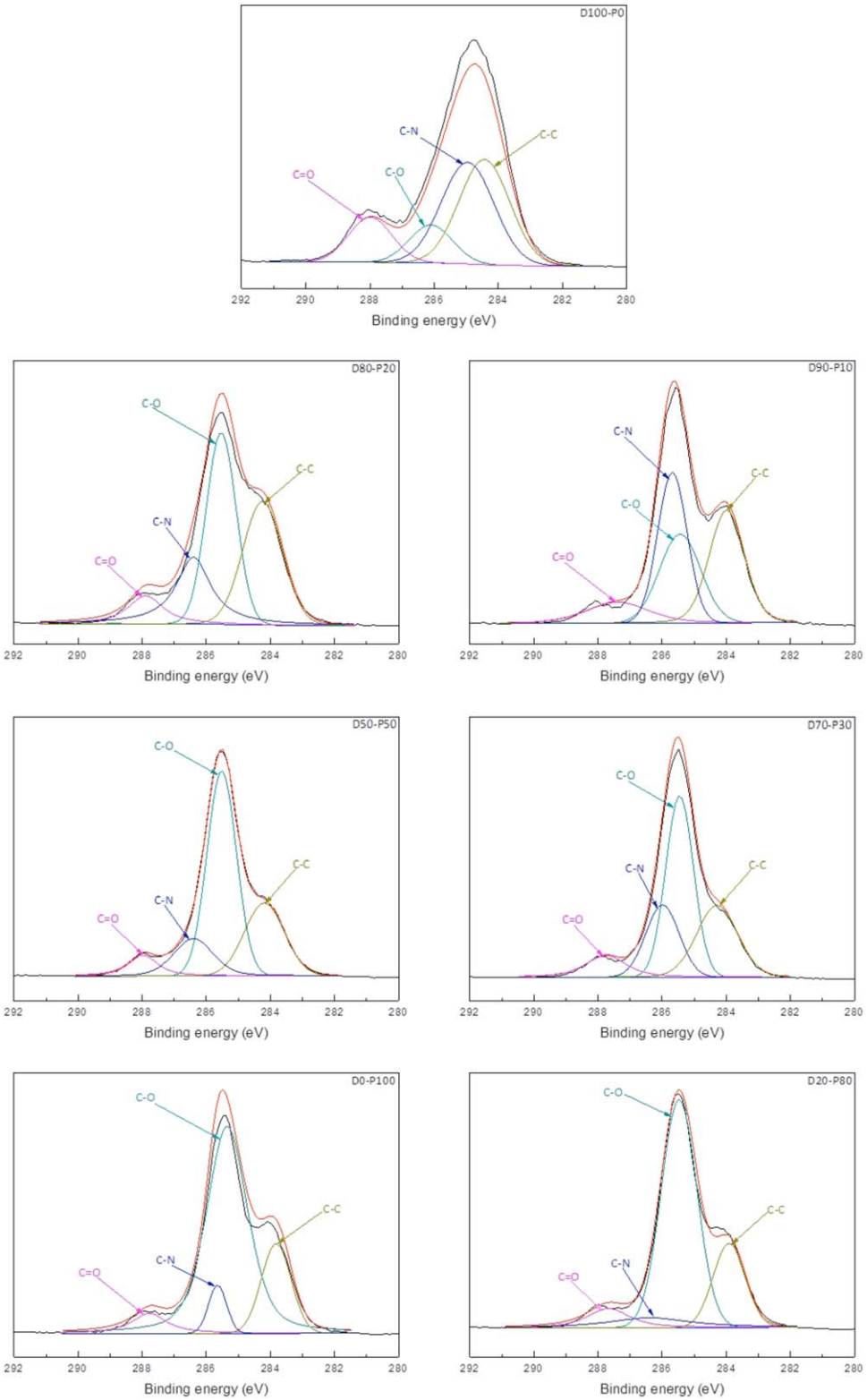

Figure 2. Curve fitting of the C 1s core-level spectra for the hydrogels. [Color figure can be viewed in the online issue, which is available at wileyonlinelibrary.com.]

the hydrogel becomes less hydrophilic as evidenced by the decline in the value of the diiodomethane contact angle. This suggests that PEGMA is more hydrophilic than DMAEMA and might be a good material to enhance the biocompatibility of hydrogels.[40] The relative fibrinogen adsorption of pure PEGMA is negligible when compared with other hydrogels. The results

Table III. Relative Abundance of Different Carbon Bonds Fitted from the XPS C 1s Core Level Spectra

	Actual						Theoretical	
Sample ID	C—O	C=O	C—C	C—N	C—O/C—N	C=O/C—N	C—O/C—N	C=O/C—N
D0-P100	0.6908	0.0691	0.1809	0.0592	11.6667	1.1667	13.1690	1.2316
D20-P80	0.6168	0.0841	0.2056	0.0935	6.6000	0.9000	8.1824	0.8923
D50-P50	0.5273	0.0727	0.2545	0.1455	3.6250	0.5000	3.9412	0.6037
D70-P30	0.4298	0.0992	0.2645	0.2066	2.0800	0.4800	2.1591	0.4823
D80-P20	0.3695	0.0887	0.3202	0.2217	1.6667	0.4000	1.7778	0.4342
D90-P10	0.2645	0.1106	0.3044	0.3206	0.8249	0.3448	0.8323	0.3921
D100-P0	0.1148	0.1372	0.3732	0.3748	0.3064	0.3660	0.2897	0.3551

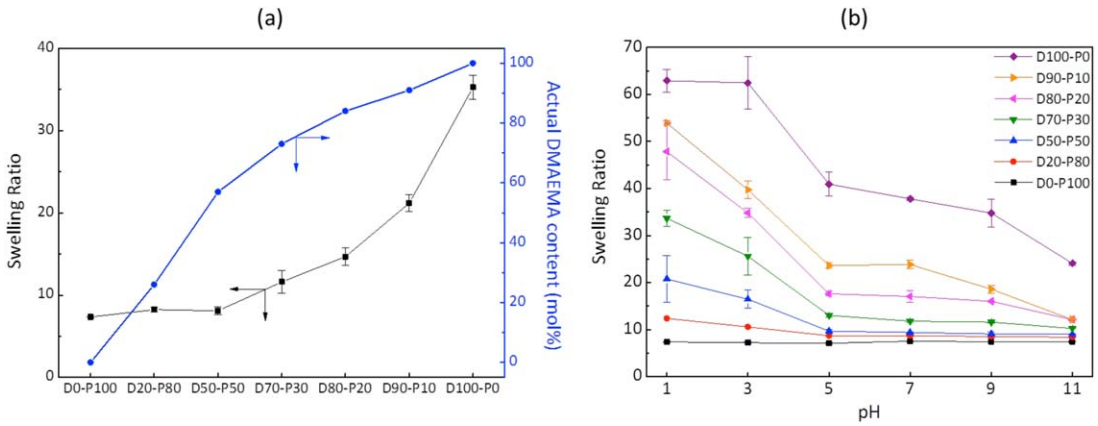

Figure 3. Swelling ratio of the hydrogels: (a) swelling ratio in DI water and actual composition of hydrogels, and (b) response of swelling ratio to the increase in pH and increase in DMAEMA content. [Color figure can be viewed in the online issue, which is available at wileyonlinelibrary.com.]

also show a sharp change in protein adsorption when increasing the PEGMA content in the hydrogels. A slight increase in DMAEMA content of the hydrogel can lead to a drastic decrease in biocompatibility. Based on the protein adsorption alone, D70-P30 has the highest potential for biomaterial applications because of its low fibrinogen adsorption.

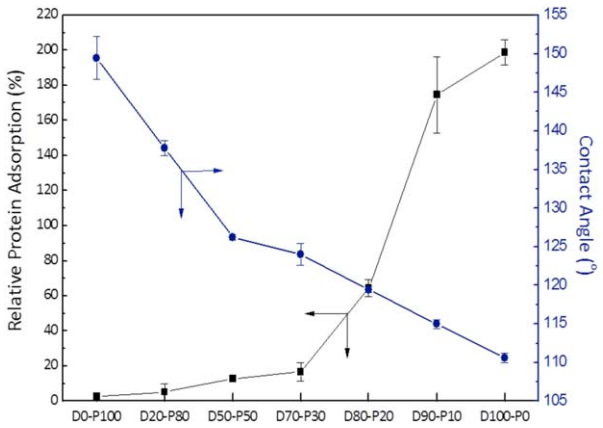

Figure 4. Correlation between nonspecific protein adsorption, hydrophilicity, and composition of dual-functional hydrogels. [Color figure can be viewed in the online issue, which is available at wileyonlinelibrary.com.]

Blood Cell Attachment and Platelet Adhesion

In this work, the intended application of the hydrogels is the controlled release of insulin. Therefore, another important characteristic to consider is their hemocompatibility. Blood incompatibility can mediate blood cell attachment, leading to blood clotting and cell lysis. Hemocompatibility of the hydrogels was measured by determining the amount of red blood cells (RBCs) adhering onto the surface of the hydrogel. Figure 5(a) shows confocal images of the hydrogels with the attached RBCs, which can be seen as green spots. To supplement these data, Figure 5(b) shows the number of RBCs attached per unit surface area of hydrogel. The results evidence that all gels containing PEGMA moieties (from D0-P100 to D70-P30) present improved hemocompatibility when compared with pure DMAEMA hydrogel, which has to be correlated with the antifouling effect of PEGMA moieties. As there is neither attractive nor repulsive electrostatic interaction involved here, blood cells are repelled following similar mechanisms as bacteria, commonly used to test the antibiofouling properties of PEG derivatives at a microscale: the hydration layer around the ethylene glycols moieties prevents the adsorption of cells. DMAEMA alone is clearly not hemocompatible; however, if the PEGMA molar composition in the hydrogel is increased to 30% only, important improvement of biocompatibility is achieved. This was also evidenced by Figure 6, showing SEM images related to the extent of platelet adhesion onto the membranes. Hydrogel only

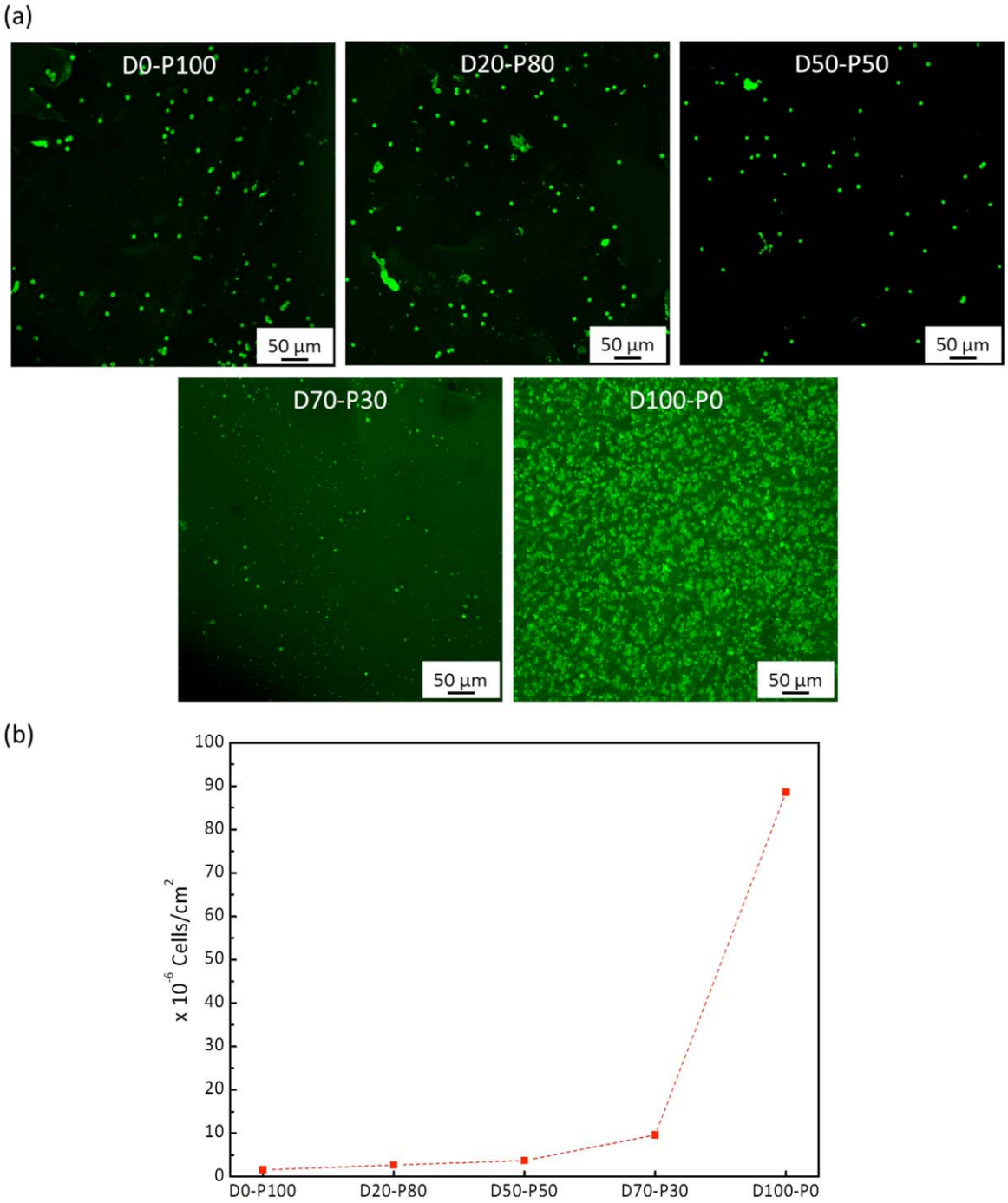

Figure 5. Effect of gel composition on red blood cells attachment at the surface of hydrogels: (a) confocal images and (b) quantitative analysis related to confocal images presented in (a). [Color figure can be viewed in the online issue, which is available at wileyonlinelibrary.com.]

containing PEGMA polymer does not present any platelet or any trace of fibrillar network arising from platelet activation. Similarly, hydrogels containing up to 50 mol % DMAEMA exhibit reduced biofouling by thrombocytes. Nevertheless, for low PEGMA content, many cells along with a dense fibrillar network can be observed at the surface of the gels. Regarding specifically resistance to platelets, the current results suggest that a minimum of 50% PEGMA in the molar composition is required to achieve low-biofouling property. Notice also that resistance to platelet can be correlated to the results related to fibrinogen adsorption (Figure 4), as this protein mediates the adhesion and activation of these cells. By integrating the results of swelling behavior, contact angle (hydrophilicity), fibrinogen adsorption, and RBC and platelet adhesion studies, it can be deduced that D70-P30 has the greatest potential for drug delivery applications. Indeed, D70-P30 has the best compromise between pH sensitivity and biocompatibility. Therefore, D70-P30 was further investigated with regards to its ability to behave as an insulin-releasing biomaterial.

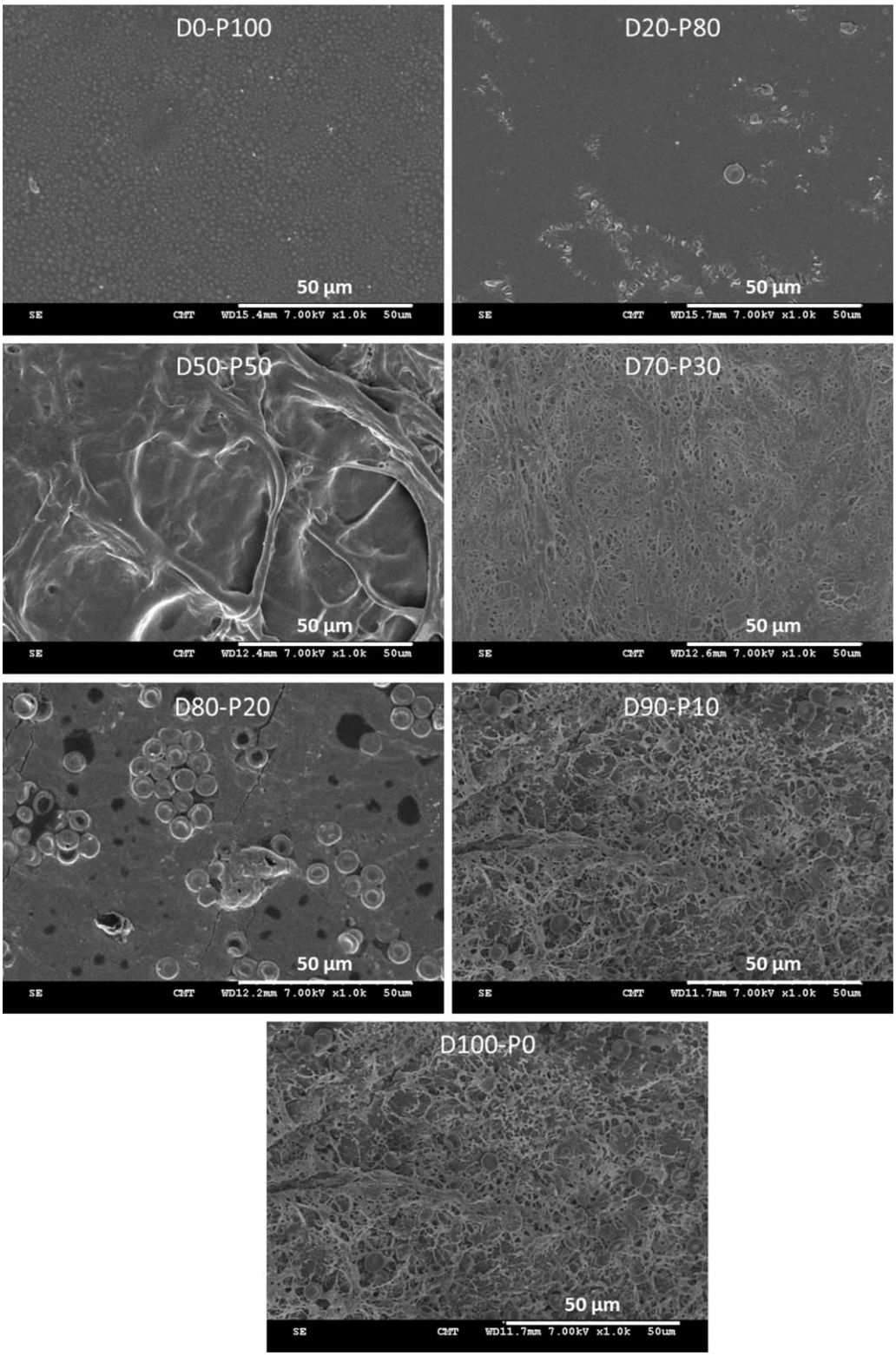

Figure 6. Effect of gel composition on platelet adhesion at the surface of hydrogels and platelet activation.

Kinetics of Insulin Release

Figure 7 presents the plot of the insulin concentration released with respect to time for all different hydrogels at pH 7.4. The data indicate that the DMAEMA:PEGMA ratio in the hydrogel affects the concentration of insulin release. As the amount of DMAEMA moieties increases, the kinetic of drug release is faster and the drug maximum concentration reaches a maximum value. It has to be associated with the stimuli-responsive

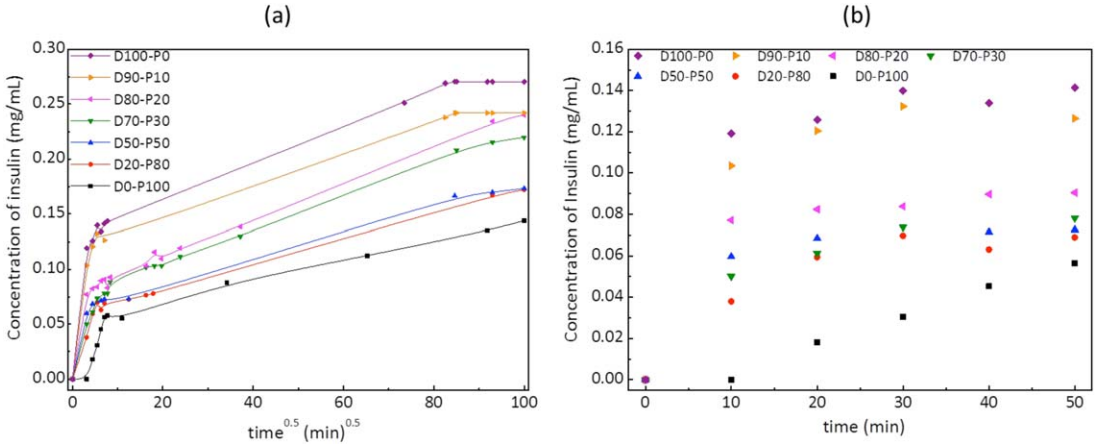

Figure 7. Kinetic of insulin release at physiological pH: (a) overall kinetic and (b) initial kinetics. [Color figure can be viewed in the online issue, which is available at wileyonlinelibrary.com.]

behavior of DMAEMA moieties. As shown earlier in Figure 3, the swelling behavior strongly depends on the composition of the hydrogels. The higher the DMAEMA content, the higher is the swelling. Swelling then facilitates drug diffusion through the polymeric network filled with water, leading to faster kinetic and higher released amount.

The release of insulin from the hydrogel can be described mathematically although the entire process is complicated and a number of different physical characteristics must be considered such as swelling, drug diffusion, polymer dissolution, axial and radial transport in a three-dimensional system, concentration-dependent diffusivities of the drug, moving boundaries, changing matrix dimensions, porosity, and composition.[41] Several models have been developed but their assumptions limit their applications.[42] A fundamental equation was derived by Korsmeyer *et al.*[43] and is still prominently used in the study of the prevailing mechanism in drug release and is now applied to D70-P30 hydrogel, which has the best compromise between biocompatibility and pH sensitivity. In the Korsmeyer–Peppas equation [eq. (2)], C_t is the insulin concentration at time t, C is the total amount of insulin, C_t/C is the fraction of insulin released at time t, k is the rate constant, and n is the exponent that can be correlated to the physical mechanism of insulin release.[43] For the hydrogel disk, the release may follow Fickian diffusion ($n \leq 0.45$); it can also be controlled by swelling ($n \approx 0.89$) or obey an anomalous non-Fickian transport ($0.45 < n < 0.89$).[44] Table IV shows the calculated release exponent values for D70-P30 as well as for D0-P100 and D100-P0 which served as controls for both lower and upper limits. The data show that the release of insulin from the hydrogel obeys Fick's second law of diffusion. A near-perfect transport sink conditions may be assumed in the case of hydrogel disks as the volume of the release medium is in large excess when compared with the volume of the disks. The boundary condition [eq. (3)] and initial condition [eq. (4)] can be applied to the hydrogel model, considering diffusion along a longitudinal axis x only, where C_i is the insulin concentration, C_o is the insulin concentration loaded inside the hydrogel, C_s is the equilibrium bulk concentration at the polymer/media interface, and R is the radius of the hydrogel. By applying the initial and boundary conditions, the solution to Fick's law can be determined from eq. (5), where D is the diffusion coefficient of insulin and C_∞ is the concentration of insulin in the bulk at equilibrium. A plot of C_t/C_∞ vs. t^5 gives a straight line, in which the slope can be used to solve for the diffusion coefficient. However, this equation is valid only during the early stages of diffusion (at the most linear part of the C_t/C_∞ vs. t^5 curve, typically for $C_t/C_\infty \leq 0.6$); however, this early stage of diffusion is suitable for studying drug transport mechanisms and release kinetics.[45] Table IV also displays the calculated diffusion coefficient at pH = 7.4 for the hydrogels studied. Note that it might be affected by the hydrogel structure and in particular the pore size of polymeric network. As insulin exists as a hexamer (MW = 34.2 kDa), at pH 6.0–7.0,[5] it is consistent with rather slow diffusivity. Clearly, increasing the amount of DMAEMA moieties in the hydrogel (D0-P100 vs. D70-P30), and thus its ability to swell, allows increasing the diffusivity of the gels and should therefore favor the release of insulin.

Table IV. Parameters Related to Diffusivity of insulin in the Different Hydrogels

Hydrogel	n[a]	Diffusion coefficient ($\times 10^{11}$ m^2 s^{-1})
D0-P100	0.40	0.17
D70-P30	0.20	0.64
D100-P0	0.12	2.3

[a] Calculated exponential value used to determine the physical mechanism for insulin release.

$$\frac{C_t}{C_\infty} = kt^n, \tag{2}$$

$$\frac{\partial C}{\partial x} = 0, \quad x = 0, \quad t > 0 \text{ and } C_i = C_s, \quad x = R, \quad t > 0, \tag{3}$$

$$C_i = C_0, \quad \text{all } x = 0, \quad t = 0, \tag{4}$$

$$\frac{C_t}{C_\infty} \cong 4\left(\frac{Dt}{\pi\delta^2}\right)^{0.5}. \tag{5}$$

One can see from Figure 7(b) that there is a rapid increase of insulin release in the initial time of kinetic (first 10 min). It

then slows down, which can be rationalized by the difference in driving force. As insulin release follows Fickian diffusion, a rapid decline in the driving force entails lower release rate. Gel composition logically strongly influences diffusivity of insulin in the matrix. As the amount of stimuli-responsive moieties increases, diffusivity increases as well. Actually, when swelling is promoted, water is the main medium through which insulin has to diffuse, whereas for low DMAEMA content, the system shrinks and insulin has to diffuse through polymeric chains. As it is well known, diffusivity in polymers lies between that in liquid and that of solid.[46] In the case of gels containing a majority of PEGMA, phenomenon at play is diffusion through a polymeric system while diffusion in liquid prevails as DMAEMA content increases, because an important quantity of liquid is entrapped between the polymeric chains.

CONCLUSIONS

This study has focused on the synthesis and characterization of poly(DMAEMA-*co*-PEGMA) hydrogels, which can function as hemocompatible and pH-sensitive biomaterial. The results show that swelling ratio of the hydrogel is directly related to the DMAEMA content and increases in an acidic pH. The result on the swelling behavior unveils that the pK_a value of the hydrogel is between 3.0 and 5.0. A number of fouling tests in static conditions were performed with proteins and blood cells, which unveiled that resistance to nanobiofouling and microbiofouling was improved as the PEGMA content in the network increased. Eventually, the hydrogel offering the best combination of swelling property and antifouling behavior, for example, D70-P30 was picked to bring insights on the potential use of such material as drug delivery system. Diffusion kinetics study using insulin as a model drug was performed, and the diffusion coefficient of insulin in this particular system was found to be 0.64×10^{-11} m^2 s^{-1} at physiological pH. In a prospective work, optimization of D70-P30 hydrogel can be investigated using enzyme immobilization technology. In particular, development of a poly(DMAEMA-*co*-PEGMA)-accommodating enzymes such as glucose oxidase with insulin is on target to better trigger the release of insulin by the pH-sensitive and hemocompatible hydrogel. In addition, the results of this study could be supplemented with *in vivo* studies using different animal models induced with diabetes mellitus.

ACKNOWLEDGMENTS

The authors thank project of Outstanding Professor Research Program in the Chung Yuan Christian University, Taiwan (CYCU-00RD-RA002-11757) and the Ministry of Science and Technology (MOST 103-2221-E-033-078-MY3) for their financial support. The Deanship of Scientific Research, College of Science Research Centre, King Saud University, Kingdom of Saudi Arabia was also supported the work.

REFERENCES

1. Uchegbu, I. F. *Expert Opin. Drug Delivery* **2006**, *3*, 629.
2. Lee, S. M.; Nguyen, S. T. *Macromolecules* **2013**, *46*, 9169.
3. Schattling, P.; Jochum, F. D.; Theato, P. *J. Polym. Sci. Part A: Polym. Chem.* **2014**, *5*, 25.
4. Loizou, E.; Triftaridou, A. I.; Georgiou, T. K.; Vamvakaki, M.; Patrickios, C. S. *Biomacromolecules* **2003**, *4*, 1150.
5. Brahim, S.; Narinesingh, D.; Guiseppie-Ellie, A. *Biomacromolecules* **2003**, *4*, 1224.
6. Fournier, D.; Hoogenboom, R.; Thijs, H. M. L.; Paulus, R. M.; Shubert, U. S. *Macromolecules* **2007**, *40*, 915.
7. Lin, S.; Du, F.; Wang, Y.; Ji, S.; Liang, D.; Yu, L.; Li, Z. *Biomacromolecules* **2008**, *9*, 109.
8. Cerda-Cristerna, B. I.; Cottin, S.; Flebus, L.; Pozos-Guillén, A. *Biomacromolecules* **2012**, *13*, 1172.
9. Zhu, C.; Zheng, M.; Meng, F.; Mickler, F. M.; Ruthardt, N.; Zhu, X.; Zhong, Z. *Biomacromolecules* **2012**, *13*, 769.
10. Nelson, C. E.; Kintzing, J. R.; Hanna, A.; Shannon, J. M.; Gupta, M. K.; Duvall, C. L. *ACS Nano* **2013**, *7*, 8870.
11. Zhu, Y.; Tang, G. P.; Xu, F. J. *ACS Appl. Mater. Interfaces* **2013**, *5*, 1840.
12. Lundy, B. B.; Convertine, A.; Miteva, M.; Stayton, P. S. *Bioconjugate Chem.* **2013**, *24*, 398.
13. Cho, H. Y.; Averick, S. E.; Paredes, E.; Wegner, K.; Averick, A.; Jurga, S.; Das, S. R.; Matyjaszewski, K. *Biomacromolecules* **2013**, *14*, 1262.
14. Lee, K. S.; In, I.; Park, S. Y. *Appl. Surf. Sci.* **2014**, *313*, 532.
15. Li, H.; Miteva, M.; Kirkbride, K. C.; Cheng, M. J.; Nelson, C. E.; Simpson, E. M.; Gupta, M. K.; Duvall, C. L.; Giorgio, T. D. *Biomacromolecules* **2015**, *16*, 192.
16. Tsai, W. B.; Grunkemeier, J. M.; Horbett, T. A. *J. Biomed. Mater. Res.* **1999**, *44*, 130.
17. Grunkemeier, J. M.; Tsai, W. B.; Alexander, M. R.; Castiner, D. G.; Horbett, T. A. *J. Biomed. Mater. Res.* **2000**, *51*, 669.
18. Corum, L. E.; Eichinger, C. D.; Hsiao, T. W.; Hlady, V. *Langmuir* **2011**, *27*, 8316.
19. Venault, A.; Wu, J. R.; Chang, Y.; Aimar, P. *J. Membr. Sci.* **2014**, *470*, 18.
20. Venault, A.; Ballad, M. R. B.; Liu, Y. H.; Aimar, P.; Chang, Y. *J. Membr. Sci.* **2015**, *477*, 101.
21. Rana, D.; Matsuura, T. *Chem. Rev.* **2010**, *110*, 2448.
22. Qiu, Y.; Park, K. *Adv. Drug Delivery Rev.* **2001**, *53*, 321.
23. Zhao, C.; Nie, S.; Tang, M.; Sun, S. *Prog. Polym. Sci.* **2011**, *36*, 1499.
24. Dupin, D.; Rosselgong, J.; Armes, S. P. *Langmuir* **2007**, *23*, 4035.
25. Sáez-Martínez, V.; Perez-Alvarez, L.; Merrero, M. T.; Hernaez, E.; Katime, I. *Eur. Polym. J.* **2008**, *44*, 1309.
26. Kim, B.; Shin, Y. *J. Appl. Polym. Sci.* **2007**, *105*, 3656.
27. Ratner, B. D.; Bryant, S. *J. Annu. Rev. Biomed. Eng.* **2004**, *6*, 41.
28. Ishihara, K.; Matsui, K. *J. Polym. Sci., Part C: Polym. Lett.* **1986**, *24*, 413.
29. Albin, G. W.; Horbett, T. A.; Miller, S. R.; Ricker, N. L. *J. Controlled Release* **1987**, *6*, 267.

30. Podual, K.; Peppas, N. A. *Polym. Int.* **2005**, *54*, 581.
31. Parker, R. S.; Doyle, F. J., III; Peppas, N. A. *IEEE Trans. Biomed. Eng.* **1999**, *46*, 148.
32. Cao, X.; Lai, S.; Lee, L. *J. Biomed. Microdevices* **2001**, *3*, 109.
33. Misra, G. P.; Siegel, R. A. *J. Controlled Release* **2002**, *81*, 1.
34. Dhanarajan, A. P.; Siegel, R. A. *Macromol. Symp.* **2005**, *227*, 105.
35. Kang, S. I.; Bae, Y. H. *J. Controlled Release* **2003**, *86*, 115.
36. Siegel, R. A.; Gu, Y.; Baldi, A.; Ziaie, B. *Macromol. Symp.* **2004**, *207*, 249.
37. Suzuki, H.; Kumagai, A. *Biosens. Bioelectron.* **2003**, *18*, 1289.
38. Chang, Y.; Yandi, W.; Chen, W.; Shih, Y.; Yang, C.; Chang, Y.; Ling, Q.; Higuchi, A. *Biomacromolecules* **2010**, *11*, 1101.
39. Kowalonek, J.; Kaczmarek, H.; Bajer, D. *Macromolecules* **2010**, *295*, 114.
40. Stine, R.; Pishko, M. V. *Langmuir* **2005**, *21*, 11352.
41. Shoaib, M. H.; Tazeen, J.; Merchant, H. A.; Yousuf, R. I. *J. Pharm. Sci.* **2006**, *19*, 119.
42. Siepmann, J.; Kranz, H.; Bodmeie, R. *Int. J. Pharm.* **2000**, *201*, 151.
43. Korsmeyer, R.; Gurny, R.; Peppas, N. *Int. J. Pharm.* **1983**, *15*, 25.
44. Siepmann, J.; Peppas, N. A. *Adv. Drug Delivery Rev.* **2001**, *48*, 139.
45. Serra, L.; Doménech, J.; Peppas, N. A. *Biomaterials* **2006**, *27*, 5440.
46. Cussler, E. L. In Diffusion Mass Transfer in Fluid Systems, 2nd ed.; Cussler, E. L. Ed.; Cambridge University Press: Cambridge, **1997**; Chapter 5, p 101.